Sheet burner nozzle: Influence of liquid mass flow and viscosity on droplet size

J. Richter[1*], M. Haas[1], T. Jakobs[1], S. Fleck[1], F. Scheiff[1,2] and T. Kolb[1,2]

*Juliana.Richter@kit.edu

[1] *Institute for Technical Chemistry, Karlsruhe Institute of Technology, Hermann-von-Helmholtz-Platz 1, 76344 Eggenstein-Leopoldshafen, Germany*

[2] *Engler-Bunte-Institute, Simulation of Reacting Thermo-Fluid Systems, Karlsruhe Institute of Technology, Engler-Bunte-Ring 7, 76131 Karlsruhe, Germany*

Abstract

High pressure entrained flow gasification (HP-EFG) is one key technology to achieve a carbon neutral circular economy by converting residual biomass and waste-based feedstocks to syngas (CO + H2), that is used for synthesis of base chemicals. Technical liquid feedstocks are often characterized by high viscosity and high heterogeneity. The fuel is atomized via a burner nozzle to maximize the free surface area for faster evaporation. According to Haas et al. [1], spray angle and droplet size have a significant impact on the amount of fuel evaporation within the reaction zone in the gasifier and thus on process efficiency. External mixing coaxial gas-assisted nozzles are commonly employed because of their superior resistance to abrasion and clogging. Due to limitations of mass flow scaling for twin-fluid nozzles, where the fuel is supplied via a central jet [2], the present study investigates liquid sheet nozzle with two coflowing gas streams.

Literature focusing on liquid sheet nozzles with two coflowing gas streams is scarce. Aiming to lay the groundwork for liquid mass flow scaling, the present work examines the influence of various liquid mass flow and liquid viscosity on droplet size, utilizing a sheet nozzle with a liquid sheet thickness of s_l = 3 mm. The investigation of droplet size was performed with a PDA system applying water (η_l = 1 mPa·s) and two glycerol/water – mixtures (η_l = 100/200 mPa·s). The droplet diameter shows a linear trend regarding the liquid mass flow, with increasing gradient for higher viscosities. Either an increase in liquid mass flow or liquid viscosity leads to larger droplet sizes. Decreasing gas-to-liquid mass flow ratio (GLR) and thus momentum flow ratio, as well as damping effects due to increased liquid viscosity explain these phenomena.

Introduction

High pressure entrained-flow gasification (HP-EFG) represents a key technology for converting residual biomass and waste-based feedstocks into synthesis gas (CO + H_2), thereby contributing to the development of a carbon-neutral circular economy. Due to the high viscosity of many technical feedstocks, efficient atomization is challenging but mandatory to maximize the liquid surface area and promote evaporation. As demonstrated by Haas et al. [1,2], spray characteristics such as droplet size and spray angle significantly affect flame zone and thus fuel evaporation. Gas-assisted nozzles are widely used in HP-EFG applications owing to their robustness. In particular, externally mixing sheet nozzles equipped with two coaxial gas streams have been proposed as promising alternatives to twin-fluid jet nozzles, Wachter et al. [3], which are often limited in scalability. The benefits of the sheet configuration with two gas streams have also been supported by Ibrahim and Jog [4] and Wahono et al. [5], as well as Leboucher et al. [6] and Wachter et al. [7], who observed enhanced primary breakup when two gas streams are employed instead of one. As a result, the sheet nozzle configuration with two gas streams is the subject of the present investigation, with focus on the influence of the liquid mass flow and liquid viscosity on the resulting droplet size.

Despite its promising potential, the literature on this specific nozzle type remains scarce, especially regarding droplet size characterization. Existing studies primarily focus on primary breakup regimes. For example, Leboucher et al. [8] introduced a breakup map plotting the total gas momentum flux against the liquid momentum flux, integrating results from Wahono et al. [5] and Fu et al. [9]. Several atomization modes are discussed in this context, including the Rayleigh breakup regime (originally

described by Kendall [10]), the bubble breakup mode (proposed by Choi and Lee [11]), and the so-called "Christmas tree" regime (introduced by Adzic et al. [12]). Only a limited number of studies have investigated droplet size distributions using this type of nozzle. Leboucher et al. [6] examined water atomization at a constant liquid mass flow rate of $\dot{M}_l$ = 39.5 kg·h^{-1} under system pressures up to 5 bar, using Phase Doppler Anemometry (PDA). The outer gas flow rate was kept constant while the inner gas stream was varied. By accounting for pressure and temperature at the nozzle exit, the gas velocities were calculated, and each operating point was designed to maintain a constant total momentum flux ratio. The results indicated that while increasing the inner gas stream significantly reduced droplet size, a rise in system pressure led to a slight increase in droplet size. Wachter et al. [7] applied PDA and used a nozzle with identical orifice areas for the inner gas, outer gas and liquid flow. This design allows for consistent momentum flows based solely on flow velocities and fluid densities. Wachter found that higher gas momentum flows generally led to smaller integral Sauter mean diameter ($Id_{32,m}$) due to increased kinetic energy available for atomization. A logarithmic dependence on liquid viscosity (η_l) was observed, where higher viscosities resulted in larger droplets. Furthermore, the outer gas stream had a more pronounced influence on droplet size than the inner one. Experiments were conducted at $\dot{M}_l$ = 30 kg·h^{-1} with viscosities ranging from η_l = 1 to 400 mPa·s. Zhao et al. [13] investigated the atomization of a water sheet across a wide range of liquid flow rates ($\dot{M}_l$ = 39 - 300 kg·h^{-1}). Their laser diffraction measurements showed that droplet sizes increased with gas velocity and corresponding mass flow rate, although the isolated effect of mass flow rate was not explicitly analyzed. While multiple operating points were tested, no direct comparison of the influence of mass flow rate was presented. However, their results confirmed that the outer gas stream exerted a much stronger impact on droplet size than the inner gas stream. Notably, at outer gas velocities ($v_{g,o}$) above approximately 40 m·s^{-1}, the inner gas stream became negligible in terms of its influence on droplet formation. Zhao et al. [13] also reported a non-monotonic relationship between outer gas velocity and droplet size, with droplet size initially increasing and then decreasing as the outer gas velocity continued to rise. This was attributed to mutual interference between the gas streams: At moderate velocities, the slower gas stream accelerates the liquid, reducing the relative velocity with the faster gas stream, which in turn leads to larger droplets. At higher velocities, the aerodynamic forces become dominant, resulting in smaller droplets.

While individual studies have examined the effect of either liquid viscosity or mass flow rate on droplet size in externally mixing sheet nozzles with two coaxial gas streams, a systematic investigation on their combined influence is not available. The present study addresses this gap by systematically analysing the combined effects of liquid mass flow rate and viscosity on droplet formation through the investigation of various mass flow rates and viscosities using a sheet nozzle with coaxial inner and outer gas flows.

Experimental Setup

Experiments were conducted using a single externally mixing sheet nozzle, featuring an inner gas exit diameter of $d_{g,i}$ = 3 mm, a liquid sheet thickness s_l = 3 mm, and an outer gas stream introduced through an annular slit with a gap width of $s_{g,o}$ = 3.1 mm. Water (η_l = 1 mPa·s) and two glycerol/water mixtures with viscosities of η_l = 100 and 200 mPa·s were used as test fluids. Surface tension (σ) and density (ρ_l) were nearly constant across all liquids (see Table 1). To minimize flow disturbance between adjacent flow passages, the separating wall thickness was reduced to b = 0.1 mm [14].

Table 1. Physical properties of all applied liquids at 20 °C and 1 atm.

	η_l in mPa·s	σ in N·m^{-1}	ρ_l in kg·m^{-3}
water	1	0.0719	998
glycerol/water (84.2 wt %)	100	0.0649	1220
glycerol/water (89.3 wt %)	200	0.0642	1233

The experimental campaign was performed using the ATMOspheric spray test rig as described in [15] and shown in Figure 1, with a high-speed camera (HSC) and a phase Doppler anemometry (PDA) system. For visualization, the high-speed camera (Phantom v1840, 2048 × 1952 pixels, 4.5 kHz) was used in combination with a backlight illumination system. Spray droplet sizes were measured using the SprayExplorer PDA system (Dantec Dynamics), operated in forward-scattering configuration and first-

order refraction mode. PDA measurements were taken at discrete radial positions across the spray, ranging from x = -60 to +60 mm. Measurements were spaced at 2 mm intervals within the central region ($-20 \leq x \leq 20$ mm), and at 5 mm intervals outside this range. At each position, droplet sizes were recorded over a period of 2 minutes to guarantee for at least 50.000 droplets. For global spray characterization, a mass-weighted integral Sauter mean diameter ($Id_{32,m}$) was determined at a fixed axial position z = 300 mm, see Equation (1). This integral value was computed as a weighted average over all radial measurement positions, based on local volume mean diameters ($D_{30,i}$), local surface mean diameters ($D_{20,i}$), local mass fluxes ($\dot{m}_i$) and the corresponding annular segment area A_i (see Figure 1 left). The calculation follows Equation 1:

$$Id_{32,\mathrm{m}} = \frac{\sum_{i=1}^{N} D_{30,i}^{3} \dot{m}_i A_i}{\sum_{i=1}^{N} D_{20,i}^{2} \dot{m}_i A_i}. \qquad (1)$$

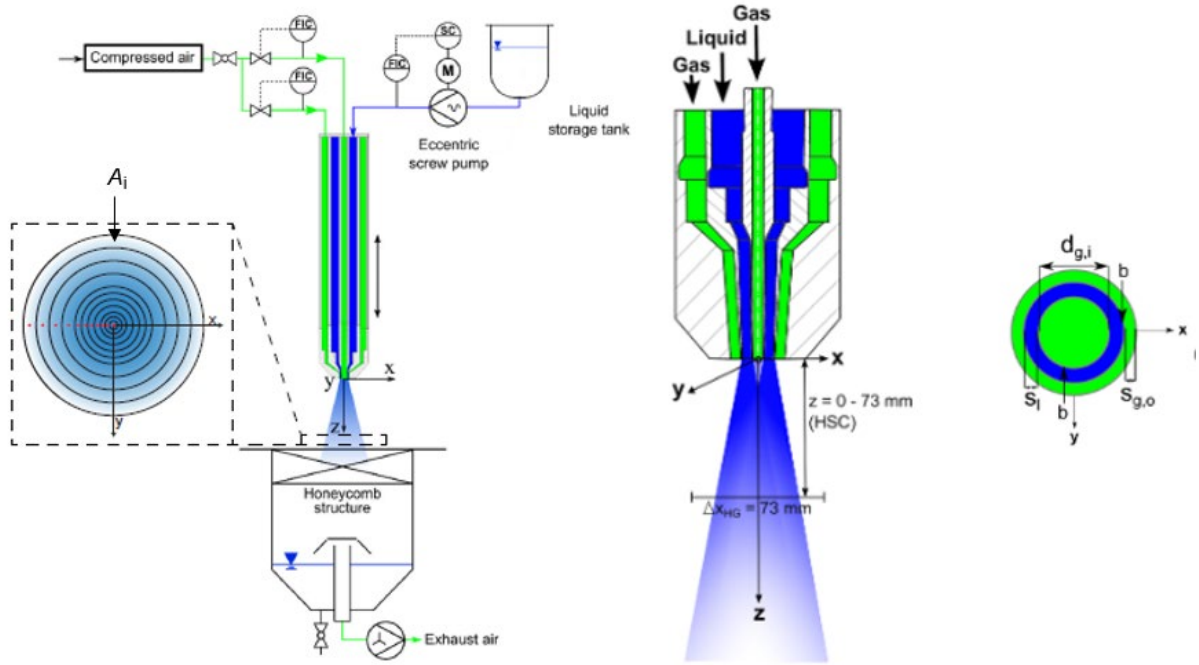

Figure 1. Schematic of the experimental setup (left). Scheme (middle) and top view of the nozzle (right).

Results and discussion

In order to investigate the influence of the liquid mass flow rate ($\dot{M}_l$) and the liquid viscosity (η_l), as well as the outer gas velocity ($v_{g,o}$), all parameters were systematically varied. The inner gas velocity ($v_{g,i}$), xx was kept constant. The influence of each parameter on droplet size was examined. The operating conditions are summarized in Table 2:

Table 2. Operating conditions of the experiments.

η_l in mPa·s	$\dot{M}_{g,i}$ in kg·h^{-1}	$v_{g,i}$ in m·s^{-1}	$\dot{M}_l$ in kg·h^{-1}	v_l in m·s^{-1}	$\dot{M}_{g,o}$ in kg·h^{-1}	$v_{g,o}$ in m·s^{-1}
1	2	65	60	0.3	24 - 72	46 - 137
1 / 100 / 200	2	65	20 - 100	0.1 – 0.5	68	130

with velocity v and mass flow rate $\dot{M}$. The indices l, g, i and o represent liquid, gas, inner or outer.

Figure 2 (top) shows that increasing the liquid viscosity from η_l = 1 to 200 mPa·s significantly increases the Sauter mean diameter across the spray, particularly at the outer boundary. This confirms the well-known trend — frequently reported in the literature [3, 6, 7, 15] — that droplets tend to be larger towards the spray periphery, where relative velocities and shear forces are lower, limiting further breakup. The corresponding high-speed images (Fig. 2, bottom) visually support this behavior by

showing distinctly larger droplets at $\eta_l = 200$ mPa·s. Contrary to common findings, only a slight increase in primary breakup length is observed at higher viscosity (Fig. 2 bottom). This can be explained by the strong aerodynamic forces at the nozzle exit, which dominate the initial breakup process and counteract the stabilizing influence of viscosity. Further downstream, however, viscous effects become more apparent as entrainment and axial momentum exchange reduce aerodynamic forces. At low viscosity, fine droplets are sheared off directly from the liquid sheet and entrained into the gas stream. In contrast, higher viscosities lead to the detachment of thicker ligaments, which are less affected by aerodynamic forces, resulting in wider spray angle with larger droplets. For all viscosities, a local maximum in droplet size near the centerline may be attributed to the dominant momentum of the outer gas stream, due to the larger annular outlet area.

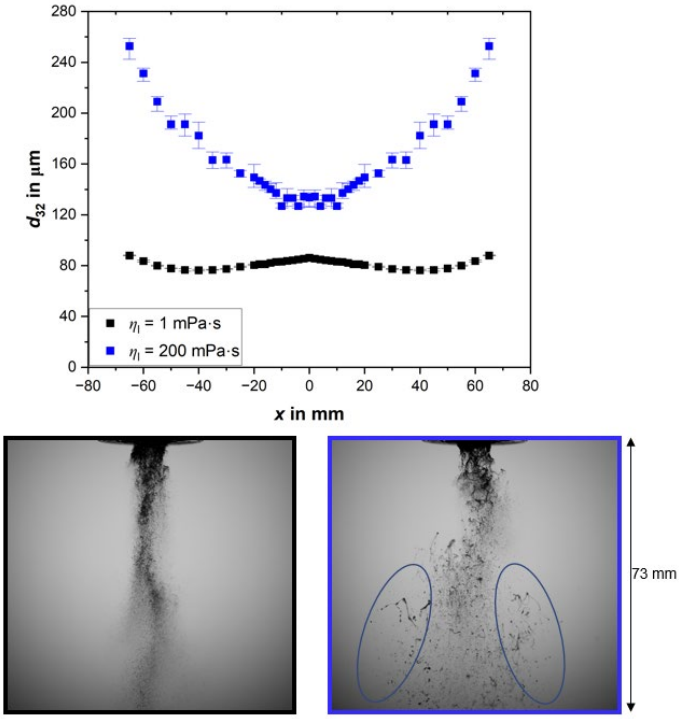

Figure 2. Top: Radial distribution of Sauter mean diameter (d_{32}) at $z = 300$ mm below the nozzle orifice as a function of liquid viscosity (η_l). Bottom: HSC images of primary sheet breakup; $\eta_l = 1$ mPa·s (left); $\eta_l = 200$ mPa·s (right). For all cases: $v_{g,i} = 65$ m·s^{-1}, $v_{g,o} = 130$ m·s^{-1}, $\dot{M}_l = 60$ kg·h^{-1}.

Although some studies suggest that the inner gas stream plays a more prominent role in promoting atomization compared to the outer stream, these conclusions are typically limited to the initial stages of primary breakup [4, 16, 17]. Other investigation [7] indicates that when both gas streams are present, the outer stream has a stronger influence on the resulting droplet size. In order to isolate the effect of the outer gas stream, the inner gas velocity ($v_{g,i}$) is kept constant while the outer velocity ($v_{g,o}$) is varied in Figure 3 (top). A pronounced decrease in mass-weighted integral Sauter mean diameter ($Id_{32,m}$) is observed with increasing $v_{g,o}$, particularly at lower velocity levels. High-speed images further confirm this trend: At $v_{g,o} = 46$ m·s^{-1} (Figure 3, bottom left), membrane-like structures form directly beneath the nozzle, evolving into ligaments and large droplets. In contrast, at $v_{g,o} = 137$ m·s^{-1} (Figure 3, bottom right), fine droplets are sheared off directly at the nozzle exit due to significantly stronger aerodynamic forces. As a result, the spray is considerably denser at higher outer gas velocities due to the presence of a large number of small droplets, compared to the fewer, larger ligaments and droplets formed at lower $v_{g,o}$.

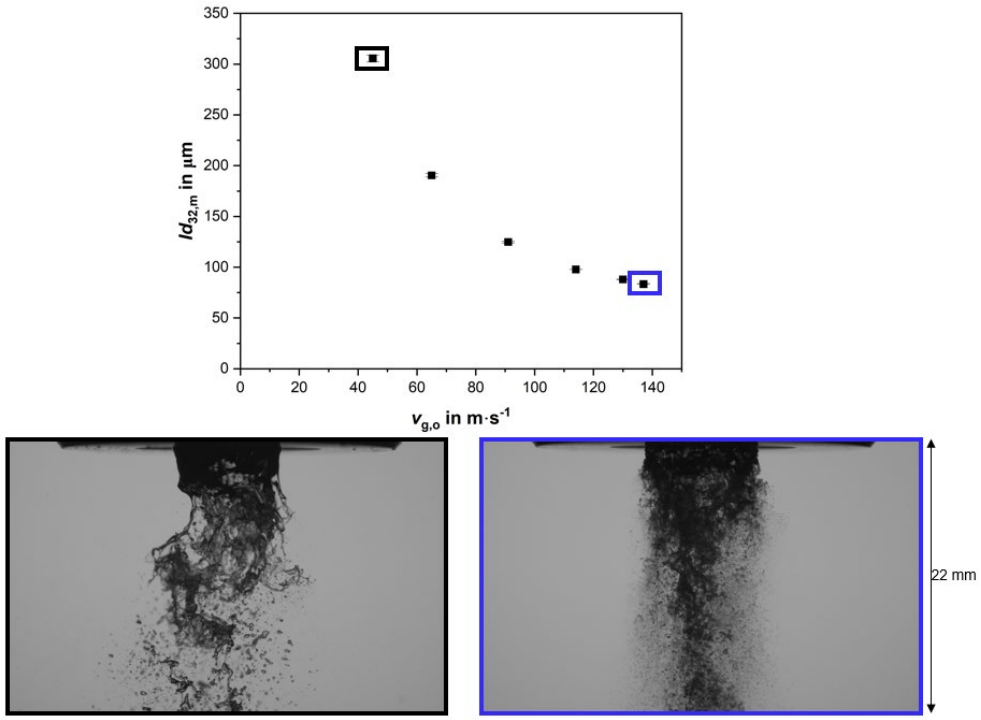

Figure 3. Top: Mass-weighted integral Sauter mean diameter ($Id_{32,m}$) at z = 300 mm below the nozzle orifice as a function of outer gas velocity ($v_{g,o}$). Bottom: HSC images of primary sheet breakup; $v_{g,o}$ = 46 m·s^{-1} (left); $v_{g,o}$ = 137 m·s^{-1} (right). For all cases: $v_{g,i}$ = 65 m·s^{-1}, $\dot{M}_l$ = 60 kg·h^{-1}, η_l = 1 mPa·s.

Finally, the influence of the liquid mass flow rate ($\dot{M}_l$) was investigated while keeping both inner and outer gas velocities constant, along with additional variation of the liquid viscosity. As shown in Figure 4 (top), the $Id_{32,m}$ increases linearly with $\dot{M}_l$, with a steeper slope observed at higher viscosities. This general trend is expected, as an increase in $\dot{M}_l$ results in higher liquid velocities, which reduce the gas–liquid momentum flux ratio and thus the effective aerodynamic shear forces acting on the liquid. The fact that $\dot{M}_l$ has a more pronounced impact on $Id_{32,m}$ at higher viscosities can be attributed to the superposition of two limiting effects: First, the increased viscosity itself requires higher aerodynamic forces to achieve comparable droplet sizes. Second, the higher mass flow reduces the gas–liquid momentum flux ratio. High-speed images at η_l = 200 mPa·s (Figure 4, bottom) for $\dot{M}_l$ = 25 kg·h^{-1} (left) and $\dot{M}_l$ = 93 kg·h^{-1} (right) show that increasing $\dot{M}_l$ leads to a wider spray, longer primary breakup lengths, and the presence of more and larger ligaments beneath the nozzle exit.

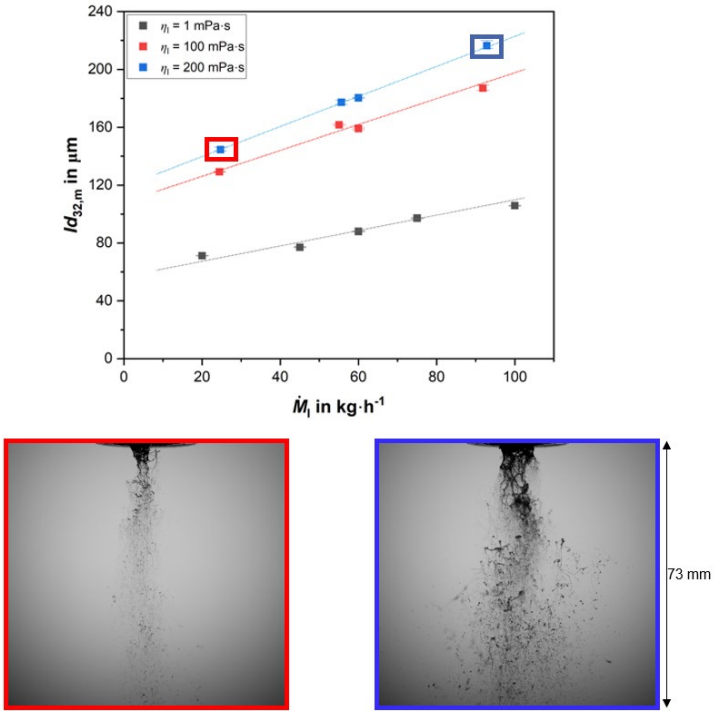

Figure 4. Top: Mass-weighted integral Sauter mean diameter ($Id_{32,m}$) at z = 300 mm below the nozzle orifice as a function of liquid mass flow rate ($\dot{M}_l$) for varying liquid viscosities (η_l). Bottom: HSC images of primary sheet breakup at η_l = 200 mPa·s, for $\dot{M}_l$ = 25 kg·h^{-1} (left) and $\dot{M}_l$ = 93 kg·h^{-1} (right). For all cases: $v_{g,i}$ = 65 m·s^{-1}, $v_{g,o}$ = 130 m·s^{-1}.

Conclusion

This study investigates the droplet formation behavior of water and two glycerol–water mixtures using a gas-assisted sheet nozzle with two coflowing gas streams. The influence of liquid viscosity (η_l), liquid mass flow rate ($\dot{M}_l$) and outer gas velocity ($v_{g,o}$) on droplet size is examined.

An increase in η_l results in larger droplets, particularly towards the outer spray boundary where shear forces are weaker. Although higher η_l generally stabilizes the liquid sheet, no substantial increase in primary breakup length is observed — likely due to the dominant aerodynamic forces near the nozzle exit. An increase in $v_{g,o}$ leads to a pronounced reduction in droplet size, especially in the lower velocity range. High-speed imaging reveals that stronger shear forces at high $v_{g,o}$ promote fine atomization, while lower $v_{g,o}$ results in the formation of thicker ligaments and larger droplets. Droplet size correlates linearly with $\dot{M}_l$, this effect is even amplified at higher viscosities. At elevated η_l and $\dot{M}_l$, the spray becomes wider, the primary breakup length increases and more prominent ligament structures are observed.

These findings establish fundamentals for liquid mass flow scaling and offer key insights into viscosity-dependent spray dynamics.

Acknowledgements

The authors gratefully acknowledge the financial support by the Helmholtz Association of German Research Centers (HGF), within the research program Materials and Technologies for the Energy Transition (MTET).

References

[1] Haas, M., Dammann, M., Fleck, S., Kolb, T.: *Entrained flow gasification: Impact of fuel spray distribution on reaction zone structure.* Fuel 334, 126572, 2023.

[2] Haas, M., Fleck, S., Jakobs, T., Kolb, T.: *Liquid fuel evaporation under entrained flow gasification conditions – insights for burner development.* Thermal Science and Engineering Progress 59, 103342, 2025.

[3] Wachter, S., Jakobs, T., Kolb, T.: *Mass flow scaling of gas-assisted coaxial atomizers*. Appl. Sci. 2123, 2022.
[4] Ibrahim, A.A., Jog, M.A.: *Nonlinear instability of an annular liquid sheet exposed to gas flow*. International Journal of Multiphase Flow 34, 2008., 2023.
[5] Wahono, S., Honnery, D., Soria, J., Ghojel, J.: *High-speed visualization of primary break-up of an annular liquid sheet*. Experiments in Fluids 44, 2008.
[6] Leboucher, N., Laporte, G., Carreau, J. L., Roger, F.: *Effect of the Inner Gas Jet on Annular Liquid Sheet Atomization.* Proc. of the 21st Annual Conf. on Liquid Atomization and Spray Systems, 2007.
[7] Wachter, S., Jakobs, T., Kolb, T.: *Comparison of central jet and annular sheet atomizers at identical gas momentum flows*. Industrial & Engineering Chemistry Research 60, 2021.
[8] Leboucher, N., Roger, F., Carreau, J.L.: *Disintegration process of an annular liquid sheet assisted by coaxial gaseos coflow(s)*. Atomization and Sprays, 2010.
[9] Fu, H., Li, X., Prociw, L., Hu, T., 2003. *Experimental investigation on the breakup of annular liquid sheets in two co-flowing airstreams*. 1st International Energy and Conversion Engineering Conference, 2003.
[10] Kendall, J.M.: *Experiments on annular liquid jet instability and on the formation of liquid shells.* Physics of Fluids 29, 1986.
[11] Choi, C.J., Lee, S.Y.:*Disintegration of annular liquid sheets with core air flow - mode classification.* ICLASS (International Conference on Liquid Atomization and Spray Systems), 1997.
[12] Adzic, M., Carvalho, I.S., Heitor, M.V.: *Visualization of the disintegration of an annular liquid sheet in a coaxial airblast injector at low atomizing air velocities*. Optics 5(1), 2001.
[13] Zhao, H., Zhao-Wei, W., Wei-Feng, L., Jian-Liang, X., Hai-Feng, L.: *Nonmonotonic effects of aerodynamic force on droplet size of prefilming air-blast atomization*. Industrial & Engineering Chemistry Research 57(5), 2018.[14]
[14] Tian, X.S., Zhao, H., Liu, H.F., Li, W.F., Xu, J.L.: *Effect of central tube thickness on wave frequency of coaxial liquid jet*. Fuel Processing Technology 119, 2014.
[15] Sänger, A., *Zerstäubung hochviskoser Fluide bei variierendem Systemdruck - Grundlagenforschung zur Hochdruck-Flugstromvergasung*, Dissertation, Karlsruher Institut für Technologie (KIT), 2018.
[16] Shen, J., Li, X.: *Breakup of annular viscous liquid jets in two gas streams. Journal of Propulsion and Power* 12, 1996.
[17] Cao, J.: *Theoretical and experimental study of atomization from an annular liquid sheet*. Proceedings of the Institution of Mechanical Engineers, Part D: Journal of Automobile Engineering 217, 2005.